

A STUDY ABOUT THE EFFECT OF CONFINING PRESSURE ON HIGH PRESSURE JET

Li Jingbin, Li Gensheng, Huang Zhongwei, Song Xianzhi
State Key Laboratory of Petroleum Resources and Prospecting, China U. of Petroleum
Beijing, Beijing 102249, China

ABSTRACT

During the drilling process for oil and gas resources, the high-pressure water jet is a key factor which can improve the rate of penetration (ROP) via breaking rock, cleaning well bore, carrying cuttings and so on. But it is always high confining pressure at the bottom of wells, which may significantly weaken the effect of high pressure water jet, especially for the deep ($\geq 4500\text{m}$) and ultra-deep ($\geq 6000\text{m}$) wells. It is crucially important to study the effect of confining pressure on high pressure water jet. A high pressure water jet simulator that could generate low confining pressure ($\leq 10\text{MPa}$) by controlling the opening of outlet valve was designed. The jet pressure and impact pressure of a classical cone nozzle with different flow rate, confining pressure, and standoff distance were measured via experiment. Results show that jet pressure hardly changes until confining pressure exceeds its 0.51 times before it linearly increases with confining pressure; numerical fitting analysis suggests that axial hydrostatic pressure is proportional to the 3.3 power of confining pressure, and increases linearly with standoff distance; axial impact pressure is inversely proportional to the 0.15 power of confining pressure, and decreases linearly with standoff distance; but when dimensionless confining pressure exceeds the threshold value which is between 0.6 and 0.7 in this research, hydrostatic pressure is in accord with confining pressure, and impact pressure won't change which means the jet is already stable. This study provides the optimization of hydraulic parameters for drilling and sand-flushing operation and the design of highly effective nozzle with helpful instructions.

1 INTRODUCTION

During the drilling process for oil and gas resources, the high-pressure water jet is a key factor which can improve the rate of penetration (ROP) via breaking rock, cleaning well bore, carrying cuttings and so on. A detailed survey funded by American National Science Foundation of over 25 novel drilling techniques revealed that hydraulic jet had the potential for drilling oil wells economically in the late 1960 s (Maurer et al. 1969).

To improve the drilling rate, the mechanism of high pressure water jet assisted rock-breaking, assembly of nozzle, optimization of fluid, structure design of nozzle, and etc. had been researched (Feenstra et al. 1964; Feenstra et al. 1973; Kolle et al. 1991; Khorshidian et al. 2014). Meanwhile, studies on velocity and pressure distribution of high pressure water jet are underway (Albertson et al. 1950; Mclean et al. 1964; Shen. 1988). But it is always high confining pressure at the bottom of wells which may tremendously weakens the effect of high pressure water jet especially for the deep ($\geq 4500\text{m}$) and ultra-deep ($\geq 6000\text{m}$) wells. Robinson (1958) researched effects of confining pressures on failure characteristics of sedimentary rocks. Brighenti (1989) reported effect of confining pressure on gas permeability of tight sandstones. Alberts (1966) evaluated the performance of two types of abrasive cutting jets in chambers that simulated ocean depths to 6100m. Surjaatmadja (2010) conducted a series of tests to define new best practices for hydrjet perforating of rock under high confining pressure. But few studies report the impact pressure attenuation of water jet under confining pressure. With the development of exploration and drilling technology, deep and ultra-deep drilling, and deepwater drilling have become the focus of drilling. It is crucially important to study the effect of confining pressure on high pressure water jet.

The impact pressure of high pressure water jet with different confining pressure is measured by experiment. The exact expression of hydrostatic pressure and impact pressure with confining pressure and standoff distance are derived by numerical fitting analysis. This study provides the optimization of hydraulic parameters for drilling and sand-flushing operation and the design of highly effective nozzle with helpful instructions.

2 FACILITIES

2.1 High Pressure Water Jet Simulator

To study the effect of confining pressure on high pressure water jet, a high pressure water jet simulator which can generate low confining pressure ($\leq 10\text{MPa}$) is designed independently. The sketch and the photo of the simulator are shown in Figure 1 and Figure 2 respectively. It mainly consists of confining pressure cylinder, nozzle, pressure tap, standoff distance adjustment lever, high pressure outlet valve. Pressure gauge and pressure sensor are simultaneously installed at two holes at the inlet and outlet for observation and accurate measurement respectively. As the main part confining pressure cylinder resists the pressure. The standoff distance adjustment lever can change distance from pressure tap to the nozzle with no interruption to experiment. The high pressure outlet valve can generate confining pressure by controlling its open. A transparent pipe is used to recycle the water. The pressure

tap connected with pressure sensor is a plane with a 1mm diameter hole in the center. This method to generate confining pressure is generally adopted in studies on confining pressure (Feenstra et al. 1973; Alberts et al; 1996; Surjaatmadja et al. 2010).

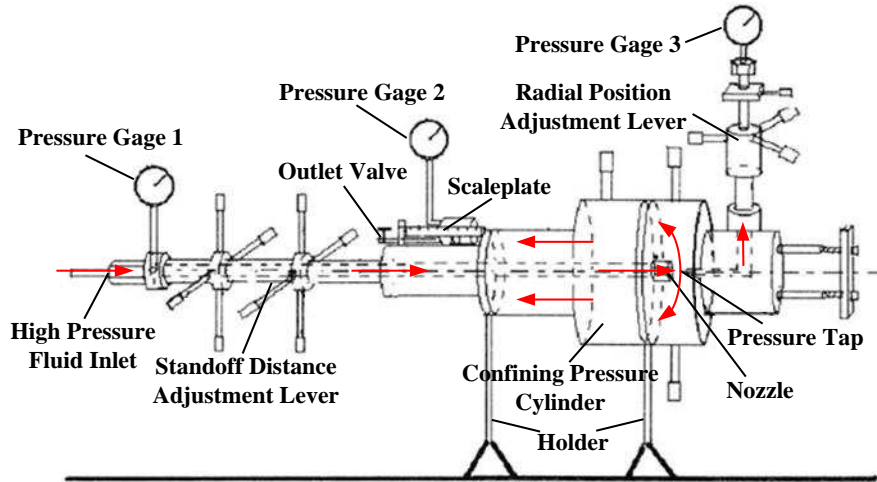


Figure 1. Sketch of High Pressure Water Jet Simulator



Figure 2. Photo of High Pressure Water Jet Simulator

2.2 Measurement Principle

As is shown in Figure 1, high pressure water flows through the inlet into the simulator and issues from the nozzle. The pressure gauge 1 and pressure sensor 1 which are installed close to the nozzle show and record the jet pressure labeled as P_1 . After that, high velocity water impacts on the pressure tap, and total pressure labeled as P_3 is obtained by pressure sensor 3. At the end, water flows through the high pressure outlet valve which generates confining pressure. Confining pressure labeled as P_c is displayed and recorded by pressure gauge 2 and pressure sensor 2. According to the theorem of momentum (Yuan. 1986), impact pressure on a plane can be calculated by:

$$P_{\text{impact}} = \rho v^2 \quad (1)$$

Then the total pressure obtained by pressure sensor 3 can be expressed as:

$$P_3 = P_{\text{static}} + P_{\text{impact}} = P_{\text{static}} + \rho v^2 \quad (2)$$

2.3 Apparatus

A high-pressure plunger pump is used as the power source with a rated pressure of 60 MPa and a certified capacity of 100 L/min. A hydro-pressure sensor with a measuring range of 30 MPa, an output current of 4~20 mA, and an accuracy of 0.1% F*S is used to measure the pressure. A 10 MPa pressure gauge and a 30MPa pressure gauge are used to read the pressure. A high-pressure valve is used to control the confining pressure. A data acquisition system in which the National Instruments multi-channel data acquisition card is installed is used to collect and store the pressure data (Figure 3). Because the purpose of experiment is to investigate the effect of confining pressure on impact pressure, the general cone nozzle is the most suitable. The nozzle has an equivalent diameter of 3mm, contraction angle of 120 °, and outlet cylindrical section of 5mm. To ensure concentricity of the nozzle and the pressure taps, the inlet of cone nozzle connected with the inflow pipe with a compress cap and a O-ring seal is designed as a conical surface, as shown in Figure 4.

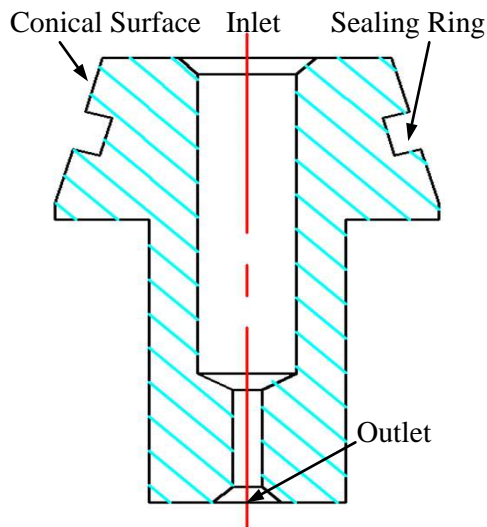
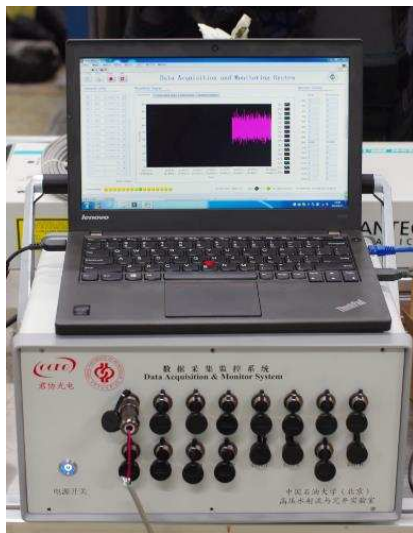


Figure 3. Multi-channel Data Acquisition System Figure 4. Sketch of Cone Nozzle

2.4 Projects

To study the impact pressure attenuation of high pressure water jet, flow rates are set as 0.6217, 0.6717, 0.7717L/s. Standoff distances are set as 1 to 7 times the nozzle diameter and are marked as 1d, 2d, 3d, 4d, 5d, 6d, 7d. Confining pressures are set as 0, 1, 2, 3, 4, 5, 6, 7MPa. All pressure data at different flow rates with different confining pressure and standoff distance are stored in the data acquisition system.

3 ANALYSES OF EXPERIMENT RESULTS

3.1 Validation

To validate the experiment method, the total pressure P_3 obtained without confining pressure is analyzed. According to Eq. 1, velocities at different standoff distance with different flow rates are obtained. The dimensionless axial velocity-dimensionless standoff distance plot is given in Figure 5. As is shown, the ordinate axis is the ratio of the measured axial velocity and the maximum axial velocity. Horizontal axis is logarithmic ratio of standoff distance to the nozzle diameter. The attenuation trends of the axial velocity with different flow rates are in good consistency with each other. According to Albertson's (1950) study, the intersection of two lines indicates the end of the potential core. The length of the potential core is about 4.6 times the nozzle diameter, which agrees with the fact very well. In conclusion, the experiment method is reliable to measure the impact pressure.

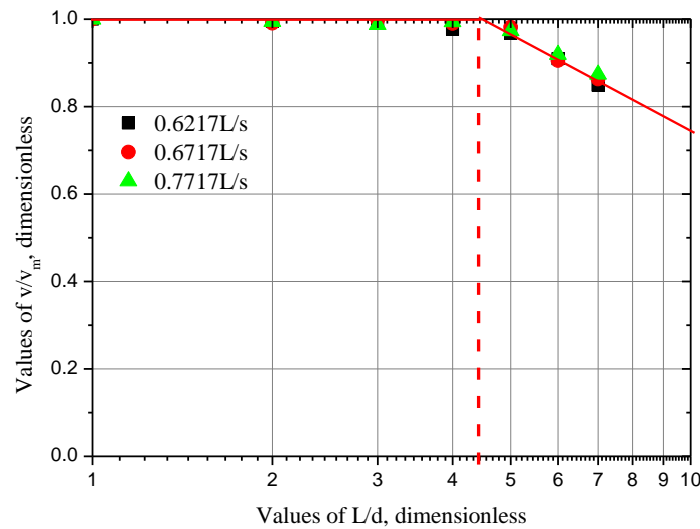


Figure 5. Axial Velocity of High Pressure Water Jet without Confining Pressure

3.2 Effect of Confining Pressure on Jet Pressure

According to the fluid dynamic energy equation, pressure drop of the nozzle (Chen et al. 2006) can be expressed as

$$\Delta P = \frac{0.05 \rho Q^2}{C^2 A^2} \quad (3)$$

According to Eq. 3, pressure drop of a special nozzle is constant for a certain flow. During the experiment, the pressure drop labeled as P_0 is equal to the jet pressure without confining pressure for different flow rates. Relationship between jet pressure and confining pressure is given in Figure 6. The ordinate axis is the ratio of measured pressure (P_3) to pressure drop (P_0). The horizontal axis is the ratio of confining pressure (P_c) to pressure drop (P_0). According to submerge theory of high pressure water jet without confining pressure, the

hydrostatic pressure in the flow field equals to environmental pressure. It can be inferred that at any cross-section of water jet the hydrostatic pressure is the same, as well as the axial direction (Shen, 1998). According to the law of conservation of energy, the jet pressure should linearly increase with the confining pressure. In fact, as is shown in Figure 6, jet pressure hardly changes until confining pressure exceeds its 0.51 times before it linearly increases with confining pressure. The effect of confining pressure on high pressure jet is complicated and needed to be further studied.

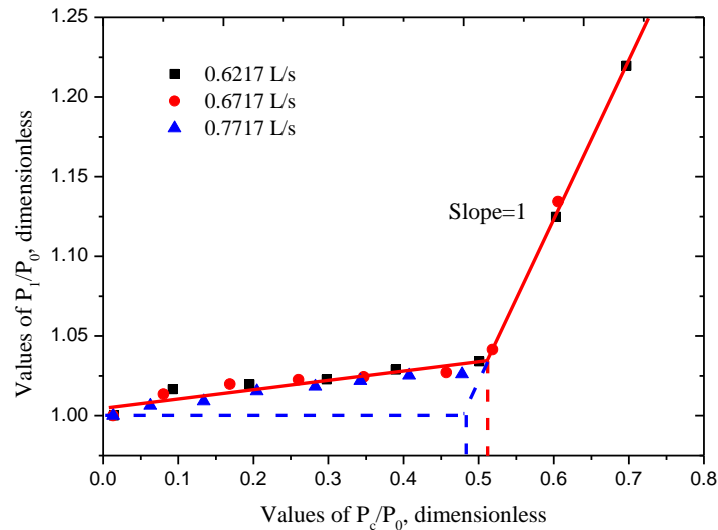


Figure 6. Effect of Confining Pressure on Jetting Pressure

3.3 Effect of Confining Pressure on Impact Pressure

To figure out the effect of confining pressure on high pressure jet, measured pressure P_3 and confining pressure P_c curves with different flow rates are given in Figure 7, Figure 8, and Figure 9 respectively. According to Eq. 2, measured pressure P_3 equals to the sum of hydrostatic pressure and impact pressure. It is easy to understand that hydrostatic pressure will increase with confining pressure which accelerates the attenuation of impact pressure. The variation of measured pressure P_3 is complex, but the slope of curves won't exceed 1. As shown in figures, dimensionless measured pressure P_3 at 1d has the same change law with jet pressure. It can be inferred that the confining pressure has no influence on high pressure jet within the standoff distance equals to 1 times nozzle diameter; as the emergence of confining pressure, measured pressure P_3 decreases quickly; with the increase of confining pressure, gradually the measure pressure P_3 stops decreasing but increases slowly instead; when the dimensionless confining pressure exceeds 0.51, measured pressure P_3 increases rapidly; as confining pressure continues to increase, the change of measured pressure tends to be linear with a 1:1 slope, which means flow field of water jet is already stable; there is a dotted line with a 1:1 slope for reference in each figure; the slope of measured pressure P_3 curve is obviously larger than 1 at the terminal section that is different with the previous analysis. We can tell that hydrostatic pressure is not evenly distributed; after dimensionless confining pressure exceeds the threshold which is in the range of 0.6~0.7 in our study, water jetting is already stable, and the measured pressure increases linearly with confining pressure.

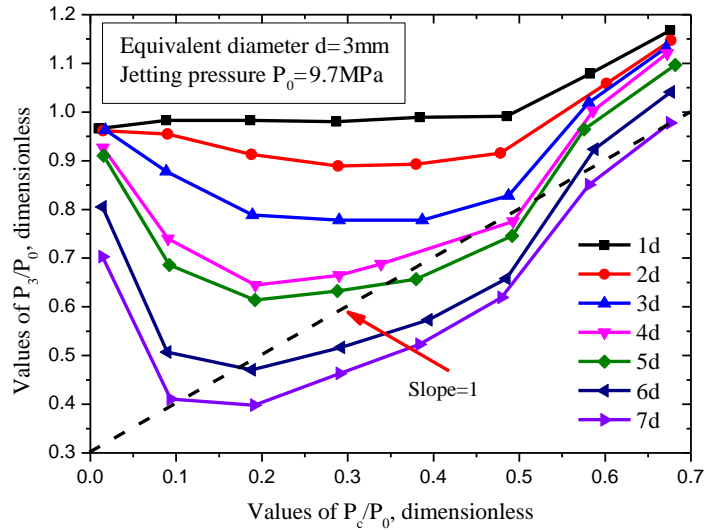


Figure 7. Effect of Confining Pressure on Measured Pressure P_3 When Flow Rate is 0.6217L/s

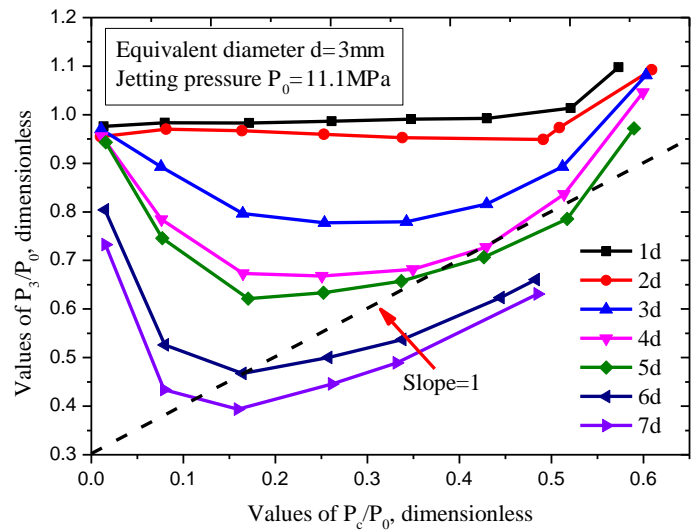


Figure 8. Effect of Confining Pressure on Measured Pressure P_3 When Flow Rate is 0.6717L/s

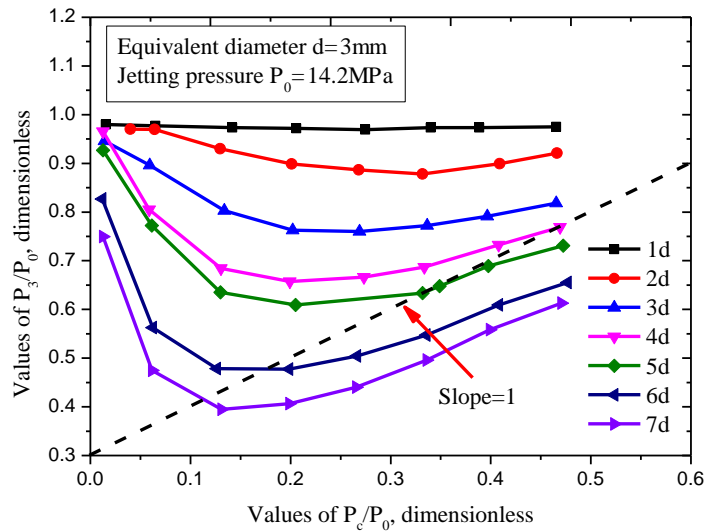


Figure 9. Effect of Confining Pressure on Measured Pressure P_3 When Flow Rate is 0.7717L/s

3.4 Numerical Fitting Analysis

To get the explicit effect of confining pressure on high pressure water jet, the measured pressure P_3 with different flow rates is summarized to Figure 10. As is shown in Figure 8, the measured pressure at 2d standoff distance differs from that in Figure 7 and Figure 9, so it is not included in Figure 10. On the basis of the analysis above, effect of confining pressure at 1d standoff distance is neglected in Figure 10, too. As shown, measured pressures with different flow rates agree with each other very well. Curves are fairly smooth which can be fitted by a single function. But when dimensionless confining pressure is larger than the threshold value, the smoothness of curves are destructed. When the dimensionless confining pressure equals to 0.7, high pressure water jet is already stable, so this part measured pressure is not considered in following parts. It is easy to understand that hydrostatic pressure is proportional to confining pressure and inversely proportional to standoff distance, while impact pressure has the opposite law. Based on above analysis, following function is used to fit the data; results are shown in Figure 11.

$$y = a * x^c + b / x^d \quad (4)$$

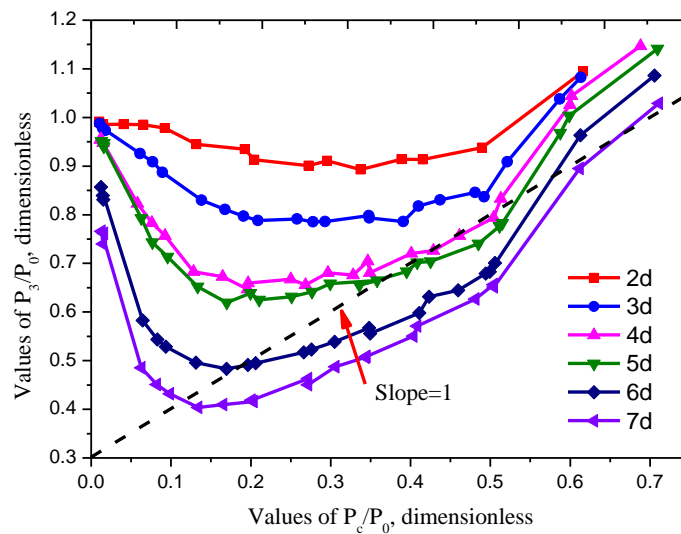


Figure 10 Effect of Confining Pressure on Measured Pressure P_3

As shown in Figure 11, the fitted curves smoothly across most of data. It proves the validity of the function which can describe the effect of confining pressure. At the same time, indexes of the function are proved to hardly change except for the 2d standoff distance. For convenience, the average of indexes is used, and Eq. 4 can be written as

$$P = a * \left(\frac{P_a}{P_0} \right)^{3.3} + b / \left(\frac{P_a}{P_0} \right)^{0.15} \quad (5)$$

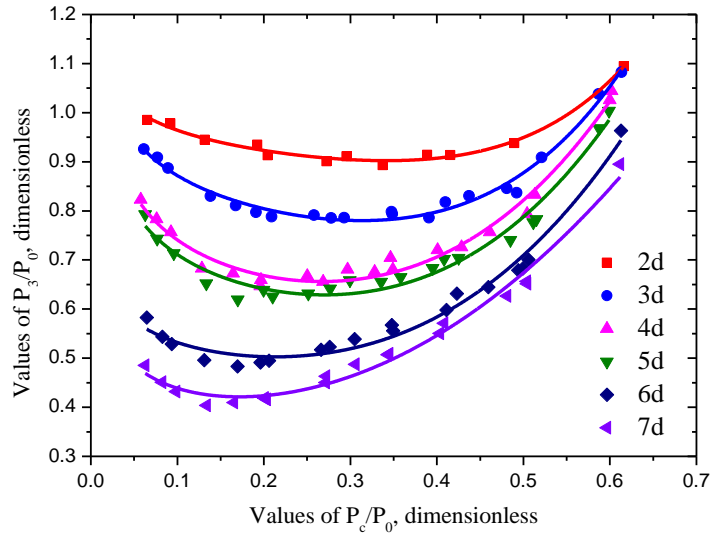


Figure 11. Results of y Function Fitting

Eq. 5 is used to fit the data again. Results are shown in Figure 12. As is shown, the fitting is preferable. The parameters of Eq. 5 turn out to be a function of dimensionless standoff distance. The fitting results are given in Figure 13. Expressions of parameters are given as follow:

$$a = 0.2244 * \frac{L}{d} + 1.371, \quad b = -0.0743 * \frac{L}{d} + 0.8413 \quad (6)$$

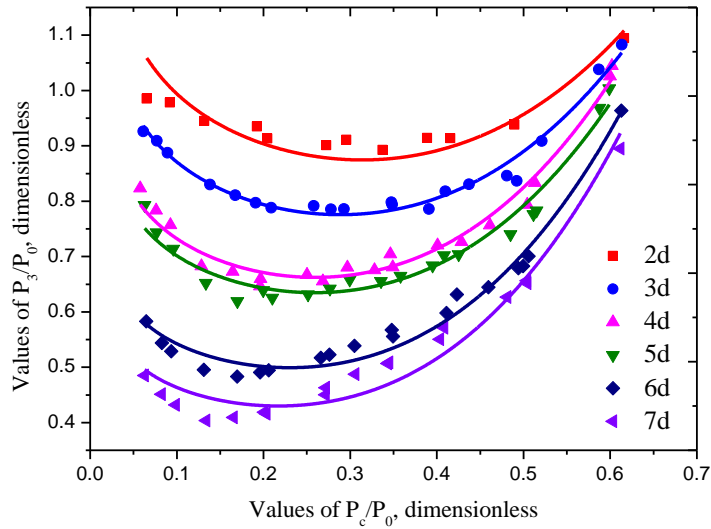


Figure 12. Results of P Function Fitting

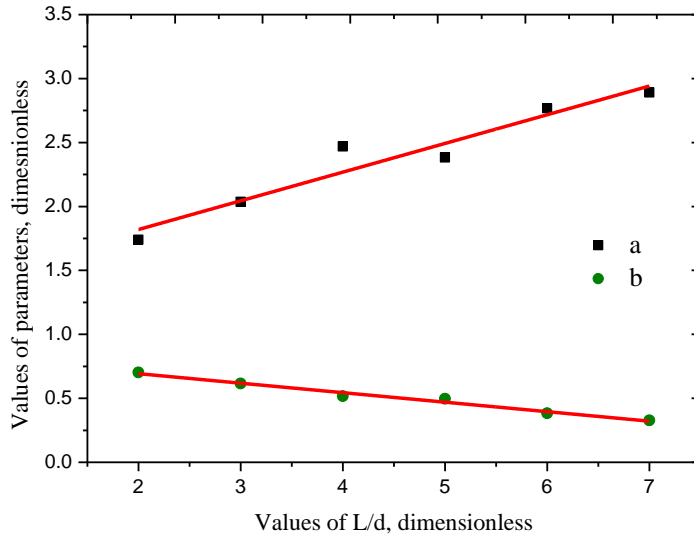


Figure 13. Results of Parameter a and b Fitting

Thus, measured pressure P_3 with different confining pressure and standoff distance can be expressed as:

$$\frac{P_3}{P_0} = \left(0.2244 * \frac{L}{d} + 1.371 \right) * \left(\frac{P_c}{P_0} \right)^{3.3} + \left(-0.0743 * \frac{L}{d} + 0.8413 \right) * \left(\frac{P_c}{P_0} \right)^{0.15} \quad (7)$$

According to Eq. 1 and Eq. 7, the distribution of hydrostatic pressure and velocity with different confining pressure and standoff distance are obtained (see Figure 14 and Figure 15).

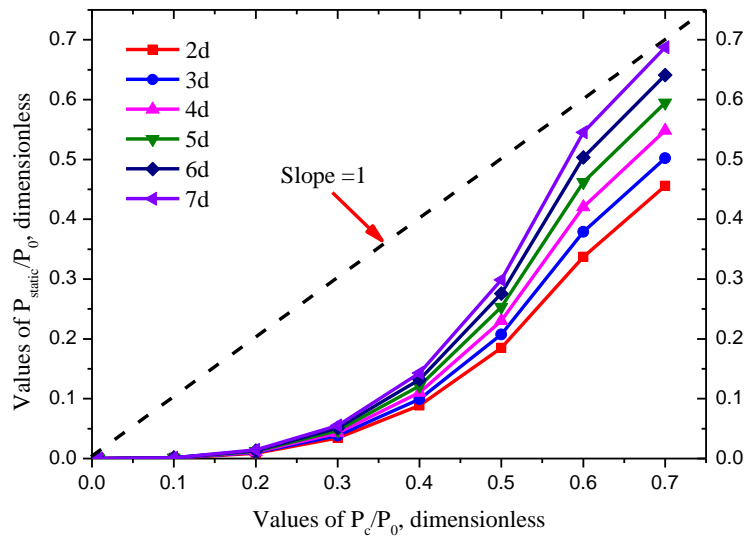


Figure 14. Changing Law of Hydraulic Static Pressure with Confining Pressure

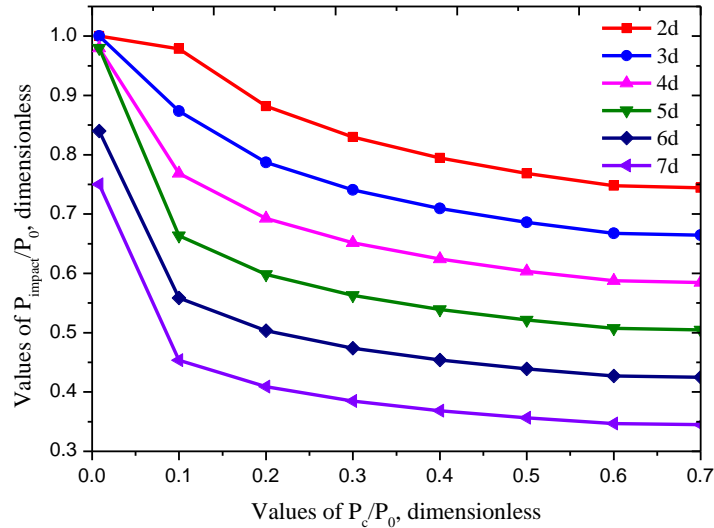


Figure 15. Changing Law of velocity with confining pressure

As shown in Figure 14, when P_c/P_0 is less than 0.2, hydrostatic pressure is tiny which is hardly affected by confining pressure; with the increase of confining pressure, hydrostatic pressure grows increasingly; when dimensionless confining pressure exceeds the threshold which is between 0.6 and 0.7 in this research, it tends to be linear with a 1:1 slope. On the contrary, impact pressure significantly decreases with confining pressure at the beginning; with the increase of confining pressure, the impact pressure attenuation gradually slows down; when dimensionless confining pressure exceeds the threshold, impact pressure basically remains unchanged, which means water jet is already stable. Figure 14 and Figure 15 explain the change law of Figure 10, which means that at the beginning of curves, the axial velocity dominates the change of measured pressure; at the end of curves hydrostatic pressure dominates the change of measured pressure.

4 CONCLUSIONS

The effect of confining pressure generated by controlling outlet valve's opening on high pressure is researched. The change law of high pressure water jet is obtained by experiment and theory analysis. The following conclusions are achieved:

(1) Jet pressure hardly changes until confining pressure exceeds its 0.51 times before it linearly increases with confining pressure.

(2) Hydrostatic pressure is not evenly distributed in the zone of high pressure jet. It is proportional to the 3.3 power of confining pressure, and increases linearly with standoff distance.

(3) Axial impact pressure is inversely proportional to the 0.15 power of confining pressure, and decreases linearly with standoff distance.

(4) There is a threshold which is between 0.6 and 0.7 in this research for dimensionless confining pressure. After that jet pressure will linear increase with confining pressure, hydrostatic pressure is in accord with confining pressure, and impact pressure won't change which means the jet is already stable.

ACKNOWLEDGMENTS

This study was funded by the National Science and Technology Major Project (No. 2011ZX05022002), the National Science and Technology Major Project (No. 2011ZX05036002) and Science Foundation of China University of Petroleum, Beijing (No. 2462013BJRC002). This support is gratefully acknowledged by the authors, who are also grateful to the reviewers of this paper for their detailed comments.

REFERENCES

- Chen Tinggen and Guan Zhichuan. Drilling Engineering Theory and Technology. Dongying : China U. of Petroleum Press, 2006. 145-146. Print.
- D.G. Alberts and M. Hashish. Evaluation of Submerged High-Pressure Waterjets For Deep Ocean Applications. The Sixth International Offshore and Polar Engineering Conference, 26-31 May, Los Angeles, California, USA. International Society of Offshore and Polar Engineers, 1 January 1996. Print.
- G. Brighenti. Effect of Confining Pressure On Gas Permeability of Tight Sandstones. ISRM International Symposium, 30 August-2 September, Pau, France. International Society of Rock Mechanics, 1 January 1989. Print.
- H. Khorshidian, S.D. Butt and F. Arvani. Influence of High Velocity Jet on Drilling Performance of PDC Bit under Pressurized Condition. The 48th U.S. Rock Mechanics/Geomechanics Symposium, 1-4 June, Minneapolis, Minnesota. Alexandria: American Rock Mechanics Association, 8 August 2014. Print.
- Jim B. Surjaatmadja, Andrew J. Bailey and Silverio A. Sierra. Hydrajet Testing Under Deep-Well Conditions Points to New Requirements for Hard-Rock Perforating. SPE Drilling & Completion 1 September 2010: 372-379. Print.
- Kolle, J.J., R. Otta and D.L. Stang. Laboratory and Field Testing of an Ultra-High-Pressure, Jet-Assisted Drilling System. Society of Petroleum Engineers, 1 January 1991: 847-857. Print.
- L.H. Robinson. Effects of Pore and Confining Pressures on Failure Characteristics of Sedimentary Rocks. The 3rd U.S. Symposium on Rock Mechanics (USRMS), 20-22 April, Golden, Colorado. Alexandria: American Rock Mechanics Association, 1 January 1959. Print.
- M. L. Albertson, Y.B. Dai, R. A. Jensen, and Hunter Rouse. Diffusion of Submerged Jets. Transactions of the American Society of Civil Engineers 1 January 1950: 639-664. Print.
- R. Feenstra and J.J.M. Van Leeuwen. Full-Scale Experiments on Jets in Impermeable Rock Drilling. Society of Petroleum Engineers, 1 March 1964: 329-336. Print.
- R. Feenstra and J. van Steveninck. Rock Cutting By Jets: A Promising Method Of Oil Well Drilling. Society of Petroleum Engineers, 1 January 1974:1-15. Print.
- R.H. McLean. Crossflow and Impact Under Jet Bits. Society of Petroleum Engineers 1 November 1964: 1299-1306. Print.
- Shen, Zhonghou and Sun Qingxiao. Study of Pressure Attenuation of a Submerged, Nonfree Jet and a Method of Calculation for Bottomhole Hydraulic Parameters. 1988. Society of Petroleum Engineers 1 March 1988: 69-76. Print.
- Shen Zhonghou. 1998. Theory and Technology of Water Jet. Dongying: China U. of Petroleum Press, 1998. 269-270. Print.
- William C. Maurer and Joe K. Heilhecker. Hydraulic Jet Drilling. Society of Petroleum Engineers, 1

January 1969: 213-217. Print.

Yuan Enxi. Engineering Fluid Mechanics. Beijing : China Petroleum Industry Press, 1986. 77-78. Print.

NOMENCLATURE

C	Nozzle discharge coefficient, dimensionless
P_{impact}	Impact pressure on the pressure tap, MPa
P_{static}	Hydrostatic pressure at the measured point, MPa
P_0	Jet pressure without confining pressure, MPa
P_1	Jet pressure measured by pressure sensor 1, MPa
P_c	Confining pressure measured by pressure sensor 2, MPa
P_3	Total pressure equals the sum of impact pressure and hydrostatic pressure, MPa
Q_i	Flow rate ($i=0, 1, 2, 3$), L/s
v	Average velocity of the outlet, m/s.
ΔP	Pressure drop of the nozzle, MPa
ρ	Density of water, Kg/m^3